Hot Subdwarf Stars and Related Objects
ASP Conference Series, Vol. 392, © 2008
U. Heber, S. Jeffery, and R. Napiwotzki, eds.

Binary sdB Stars with Massive Compact Companions

S. Geier,[1] C. Karl,[1] H. Edelmann,[2] U. Heber,[1] and R. Napiwotzki[3]

[1]*Dr.–Remeis–Sternwarte, Institute for Astronomy, University Erlangen-Nuremberg, Sternwartstr. 7, 96049 Bamberg, Germany*

[2]*McDonald Observatory, University of Texas at Austin, 1 University Station, C1402, Austin, TX 78712-0259, USA*

[3]*Centre of Astrophysics Research, University of Hertfordshire, College Lane, Hatfield AL10 9AB, UK*

Abstract. The masses of compact objects like white dwarfs, neutron stars and black holes are fundamental to astrophysics, but very difficult to measure. We present the results of an analysis of subluminous B (sdB) stars in close binary systems with unseen compact companions to derive their masses and clarify their nature. Radial velocity curves were obtained from time resolved spectroscopy. The atmospheric parameters were determined in a quantitative spectral analysis. Based on high resolution spectra we were able to measure the projected rotational velocity of the stars with high accuracy. In the distribution of projected rotational velocities signs of tidal locking with the companions are visible. By detecting ellipsoidal variations in the lightcurve of an sdB binary we were able to show that subdwarf binaries with orbital periods up to 0.6 d are most likely synchronized. In this case, the inclination angles and companion masses of the binaries can be tightly constrained. Five invisible companions have masses that are compatible with that of normal white dwarfs or late type main sequence stars. However, four sdBs have compact companions massive enough to be heavy white dwarfs ($> 1\,M_\odot$), neutron stars or even black holes. Such a high fraction of massive compact companions is not expected from current models of binary evolution.

1. Introduction

The mass of a star is its most fundamental property. However, a direct measurement is possible in a small number of binary stars only. White dwarfs, neutron stars and stellar mass black holes are the fibal products of stellar evolution. In most binaries such faint, compact objects are outshone by their bright companions and therefore their orbital motion cannot be measured. Only lower limits to the companion mass can be derived. With the analysis method shown here, these limitations can be partly overcome.

Subluminous B stars are considered to be helium core burning stars with very thin hydrogen envelopes and masses around $0.5\,M_\odot$. Different formation channels have been discussed. As it turned out, a large fraction of the sdB stars are members of short period binaries (Maxted et al. 2001). For these systems common-envelope ejection is the most probable formation channel (Han et al. 2002). In this scenario two main-sequence stars of different masses evolve in a

binary system. The heavier one will first reach the red giant phase and fill its Roche lobe. If the mass transfer to the companion is dynamically unstable, a common envelope is formed. Due to friction the two stellar cores loose orbital energy, which is deposited within the envelope and leads to a shortening of the binary period. Eventually the common envelope is ejected and a close binary system is formed, which contains a helium core burning sdB and a main sequence companion. When the latter reaches the red-giant branch, another common envelope phase is possible and can lead to a close binary with a white-dwarf companion and an sdB star. All known companions of sdB stars in such systems are white dwarfs or late-type main-sequence stars. If massive stars are involved, the primary may evolve into a neutron star (NS) or a black hole (BH) rather than a white dwarf. Since massive stars are very rare, only few sdB+NS or sdB+BH systems are expected to be found.

Since the spectra of most binary sdBs are single-lined, they reveal no information about the orbital motion of their companions, and thus only their mass functions can be calculated.

$$f_{\rm m} = \frac{M_{\rm comp}^3 \sin^3 i}{(M_{\rm comp} + M_{\rm sdB})^2} = \frac{PK^3}{2\pi G}. \quad (1)$$

Although the RV semi-amplitude K and the period P are determined by the RV curve, two of $M_{\rm sdB}$, $M_{\rm comp}$ and $\sin i$ remain free parameters. Binary population synthesis models (Han et al. 2002) indicate a possible mass range of $M_{\rm sdB} = 0.30{-}0.48\,{\rm M}_\odot$ for sdBs in binaries, which underwent the common envelope ejection channel. The mass distribution shows a sharp peak at about $0.46\,{\rm M}_\odot$. This theoretical value can be backed up by observations (Edelmann these proceedings; Vuckovic et al. these proceedings) as well as asteroseismology (e.g. Charpinet et al. these proceedings).

For close binary systems, the components' stellar rotational velocities are considered to be tidally locked to their orbital motions, which means that the orbital period of the system equals the rotational period of the companions. If the companions are synchronized in this way the rotational velocity $v_{\rm rot}$ can be calculated.

$$v_{\rm rot} = \frac{2\pi R_{\rm sdB}}{P}. \quad (2)$$

The stellar radius R is given by the mass–radius–relation.

$$R = \sqrt{\frac{M_{\rm sdB} G}{g}} \quad (3)$$

The measurement of the projected rotational velocities $v_{\rm rot} \sin i$ therefore allows us to constrain the systems' inclination angles i. With $M_{\rm sdB}$ as free parameter the mass function can be solved and the inclination angle as well as the companion mass can be derived. Because $\sin i \leq 1$, a lower limit for the sdB mass is given. To constrain the system parameters in this way it is necessary to measure K, P, $\log g$ and $v_{\rm rot} \sin i$ with high accuracy.

2. Observations and Radial Velocity Curves

Ten stars were observed at least twice with the high-resolution spectrograph UVES at the ESO VLT. Additional observations were made at the ESO NTT (equipped with EMMI), the Calar Alto Observatory 3.5-m telescope (TWIN) and the 4-m WHT (ISIS) on La Palma. Two of the stars (PG 1232−136, TONS 183) were observed with the high resolution FEROS instrument at the 2.2 m ESO telescope at La Silla. The radial velocities (RV) were measured by fitting a set of mathematical functions (Gaussians, Lorentzians and polynomials) to the hydrogen Balmer lines. Sine curves were fitted to the RV data points using a χ^2 minimising method (singular-value decomposition) and the temporal power spectrum was generated to obtain a best-fit period (Table 1).

3. Atmospheric Parameters and Projected Rotational Velocities

The spectra were corrected for the measured RV and co-added. Atmospheric parameters were determined by fitting simultaneously each observed hydrogen and helium line with a grid of metal-line blanketed LTE model spectra. Partial results are listed in Table 1.

Table 1. Surface gravities, orbital periods, radial velocity semi-amplitudes and projected rotational velocities of the visible components. The typical error margin for $\log g$ is 0.05 dex. † Orbital parameters of this system taken from Geier et al. (these proceedings). ‡ Orbital parameters of this system taken from Napiwotzki et al. (2001).

System	$\log g$ [$\mathrm{cm^2 s^{-1}}$]	P [d]	K [$\mathrm{km\,s^{-1}}$]	$v_{\rm rot}\,\sin i$ [$\mathrm{km\,s^{-1}}$]
HE 0532−4503	5.32	0.26560 ± 0.00010	101.5 ± 0.2	11.1 ± 0.6
PG 1232−136	5.62	0.36300 ± 0.00030	129.6 ± 0.04	6.2 ± 0.8
WD 0107−342†	5.32	0.37500 ± 0.05000	127.0 ± 2.0	20.4 ± 0.9
HE 0929−0424	5.71	0.44000 ± 0.00020	114.3 ± 1.4	7.1 ± 1.0
HE 0230−4323	5.60	0.44300 ± 0.00050	64.1 ± 1.5	12.7 ± 0.7
TONS 183	5.20	0.82770 ± 0.00020	84.8 ± 1.0	6.7 ± 0.7
HE 2135−3749	5.84	0.92400 ± 0.00030	90.5 ± 0.6	6.9 ± 0.5
HE 1421−1206	5.55	1.18800 ± 0.00100	55.5 ± 2.0	6.7 ± 1.1
HE 1047−0436‡	5.66	1.21325 ± 0.00001	94.0 ± 3.0	6.2 ± 0.6
HE 2150−0238	5.83	1.32090 ± 0.00500	96.3 ± 1.4	8.3 ± 1.3
HE 1448−0510	5.59	7.15880 ± 0.01300	53.7 ± 1.1	6.7 ± 2.5
WD 0048−202	5.50	7.44360 ± 0.01500	47.9 ± 0.4	7.2 ± 1.3

In order to derive $v_{\rm rot}\,\sin i$, we compared the observed spectra with rotationally broadened, synthetic line profiles. The latter were computed using the LINFOR program (Lemke 1997). Since sharp metal lines are much more sensitive to rotational broadening than Balmer or helium lines, all visible metal lines were included. A simultaneous fit of elemental abundance and projected rotational velocity was performed separately for every identified line using the

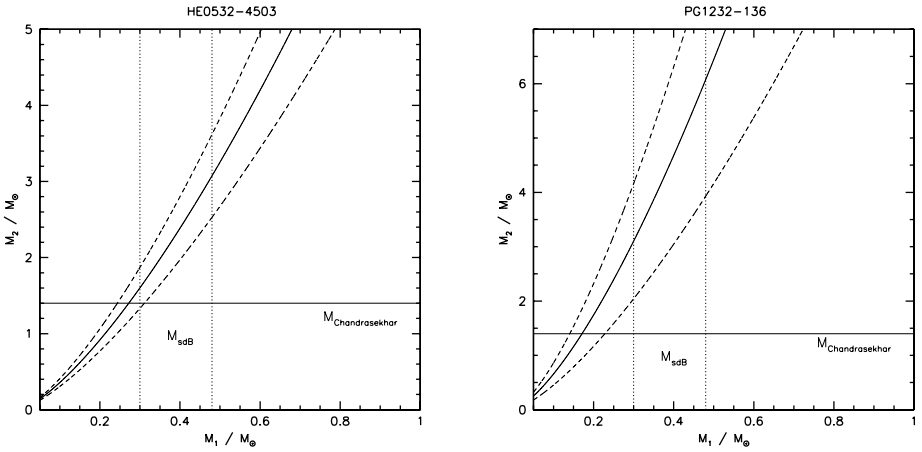

Figure 1. Companion mass as a function of primary (sdB) mass of the binaries HE 0532−4503 (left hand panel) and PG 1232−136 (right hand panel). The horizontal line marks the Chandrasekhar limit. The dotted vertical lines mark the theoretical sdB mass range for the common envelope ejection channel (Han et al. 2002).

FITSB2 routine (Napiwotzki et al. 2004). The mean value and the standard deviation were calculated from all measurements. Seeing induced variations in the instrumental profile and the noise level were the dominant error sources. Information on the actual seeing conditions for every exposure have been extracted from the ESO seeing monitor archive. All other possible sources of systematic errors turned out to be negligible.

4. Nature of the Unseen Companions

Knowing P, K, $\log g$ and $v_{\rm rot} \sin i$ we can calculate the mass of the unseen companion from Eqns. 1−3 for any given primary mass (see Fig. 1). We adopt the mass range from Han et al. (2002), marked by the dotted lines in Fig. 1. There are no spectral signatures of companions visible. Main sequence stars with masses higher than $0.45\,M_\odot$ could therefore be excluded because they would contribute to the total flux and could therefore be identified from the spectral energy distribution and/or indicative spectral features. The possible companion masses can be seen in Table 2. Four of the analysed systems have companion masses, which are compatible with either typical white dwarfs (WD) or late main-sequence stars (late MS). The companion of WD 0107−0342 is a massive white dwarf. Since the total mass of the binary may exceed the Chandrasekhar limit, the system is a good candidate for a double degenerate SN Ia progenitor with subdwarf primary, only the second one after KPD 1930+2752 (Geier et al. 2007a).

The very similar HE 0929−0424 and TONS 183 have to have quite massive companions. Even in the less likely case that their sdB primaries are of low mass ($\approx 0.3\,M_\odot$) the companions would be heavy white dwarfs. At the most probable sdB mass, however, their companions would exceed the Chan-

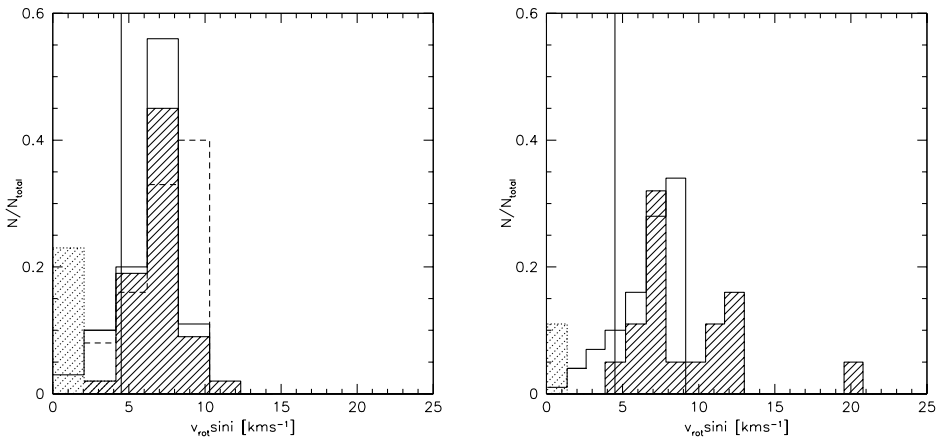

Figure 2. *Left panel:* The measured $v_{\rm rot}\sin i$ of 49 single sdBs is plotted against relative fraction of stars as shaded histogram. The solid blank histogram marks the expected uniform distribution of $v_{\rm rot}\sin i$ under the assumption of randomly oriented polar axes and uniform rotational velocity $v_{\rm rot} = 8.3\,{\rm kms}^{-1}$ for all stars. The dashed blank histogram marks a uniform distribution for $v_{\rm rot} = 9.0\,{\rm kms}^{-1}$ as comparison. All sdBs with $v_{\rm rot}\sin i$ below the detection limit (vertical line) are stacked into the first bin (dotted shaded histogram). The width of the bins is given by the average $v_{\rm rot}\sin i$ uncertainty of the sample. *Right panel:* The measured $v_{\rm rot}\sin i$ of 19 RV variable sdBs is plotted against relative fraction of stars as shaded histogram. The solid blank histogram marks the uniform distribution derived from the single star sample. The width of the bins is again given by the average $v_{\rm rot}\sin i$ uncertainty of the sample, which is lower for the RV variable sample due to better quality of the data.

drasekhar mass limit. There are only two kinds of objects known with such high masses and such low luminosities – neutron stars and stellar mass black holes. The two systems HE 0532−4503 and PG 1232−136 have even higher companion masses, which would exceed the Chandrasekhar limit for any mass of a core helium-burning subdwarf star (see Fig. 1). The three long-period binaries HE 1448−0510, HE 2150−0238 and WD 0048−202 could not be solved with the described method. These systems cannot be synchronized (see Sect. 5).

Binaries hosting a neutron star or a black hole are a very rare class of objects. From about 50 analysed sdB binaries in our samples, we found two, possibly four candidate systems. This fraction of 4–8% is much too high to be compatible with any binary evolution model known so far (Podsiadlowski priv. comm.).

Our results depend strongly on the projected rotational velocity. The unexpectedly high masses could only be reduced if the $v_{\rm rot}\sin i$ were underestimated. As described above we quantified all possible systematic effects and the overall results were very consistent. But even if there would be unaccounted systematic effects (e.g. short period pulsations), they would always cause extra broadening of the lines. The measured broadening is then due to rotation plus the unaccounted effects, which means the deduced rotational broadening would be

overestimated. Potential systematic effects yet unaccounted for would therefore lead to even higher companion masses.

5. Orbital Synchronization of sdB Binaries

Our method rests on the assumption of orbital synchronization. In Fig. 2 we compare the $v_{\rm rot} \sin i$-distribution of close sdB binaries to the distribution of the single stars. A large fraction of binary sdBs exceeds the maximum $v_{\rm rot} = 8.3\,{\rm kms}^{-1}$, derived for the single sdB stars, significantly. The most likely reason for this is tidal interaction with the companion.

The question of which mechanisms are responsible for the synchronization of such stars is not yet settled. Subluminous B stars have convective cores and radiative envelopes. The physical mechanisms for tidal dissipation in such stars are under debate. Different theoretical concepts (Zahn 1977; Tassoul & Tassoul 1992) predict that the synchronization timescale $t_{\rm sync}$ depends strongly on the orbital period but differs in absolute values. Tidal locking can only be assumed if the synchronization time scales are significantly lower than the average lifetime on the EHB of $t_{\rm EHB} \approx 10^8\,{\rm yr}$. Using the formalism of Zahn (1977) $t_{\rm sync}$ would exceed $t_{\rm EHB}$ for periods longer than $P^{\rm lim}_{\rm Zahn} \approx 0.4\,{\rm d}$, whereas this would be the case at $P^{\rm lim}_{\rm Tassoul} \approx 2.0\,{\rm d}$ if we apply the theory of Tassoul & Tassoul (1992).

But as long as the question of tidal synchronization is not settled, all timescales have to be taken with caution (Zahn 2005). Detailed calculations, which take the internal structure of sdBs into account, are not available and urgently needed. Observational constraints are necessary to guide the development of more sophisticated models.

Up to now such observational constraints are rare. Two short period ($\approx 0.1\,{\rm d}$) sdB binaries with white-dwarf companions show light variations due to their ellipsoidal deformation (Orosz & Wade 1999; Geier et al. 2007a) and are therefore most likely synchronized. Randall et al. (2005) reported the detection of shallow ellipsoidal variations in the longer period ($\approx 0.6\,{\rm d}$) sdB+WD binary PG 0101+039. Geier et al. (2008) verified that the light variations are due to ellipsoidal deformation and that tidal synchronization is very likely established for PG 0101+039 (see Fig. 3). We conclude that this assumption should hold for all sdB binaries with orbital periods of less than half a day. Last but not least, van Grootel et al. (these proceedings) carried out an asteroseismological analysis of the pulsating sdB in the binary Feige 48 (sdB+WD, $P = 0.376\,{\rm d}$) and found it to be synchronized.

In Table 2 we show which binaries fulfill the empirical or theoretical criteria for synchronization. It has to be pointed out that three of our candidate systems with massive compact companions are consistent with all of them.

6. Conclusion

Out of 12 analysed sdB binaries, five have companion masses compatible with white dwarfs of typical mass or late-type main-sequence stars. The properties of these systems are in full agreement with binary population-synthesis simulations. Four binaries have surprisingly high companion masses, which leads to the conclusion, that the companions have to be white dwarfs of unusually high mass

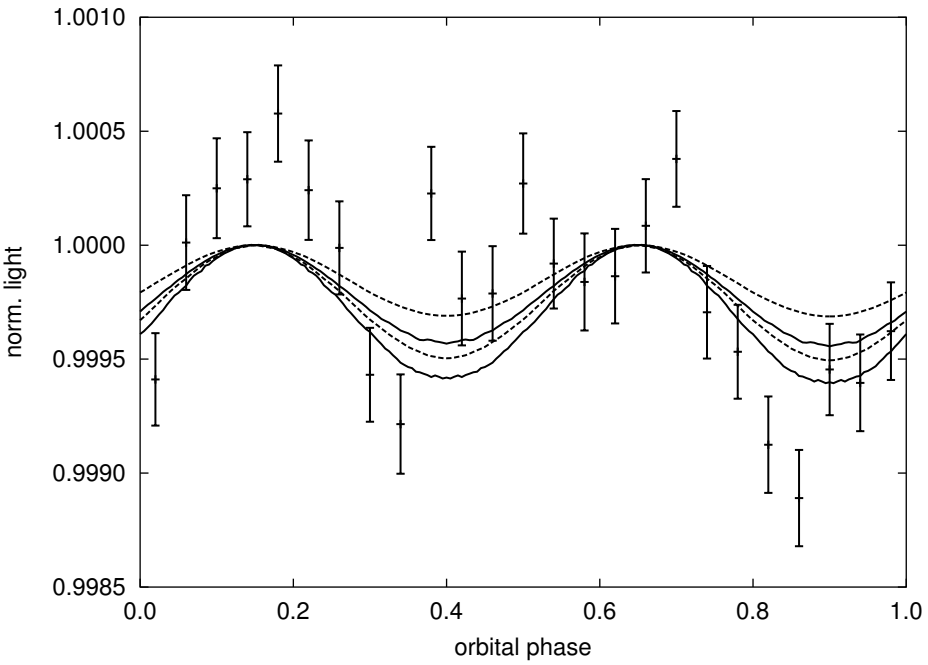

Figure 3. Lightcurve of PG 0101+039 with superimposed models (Geier et al. 2008). The two solid curves confine the best fit models with parameters and associated uncertainties derived from spectroscopy under the assumption of orbital synchronization and $M_{\rm sdB} = 0.3\,M_{\odot}$. The two dotted curves confine models for $M_{\rm sdB} = 0.7\,M_{\odot}$.

or even neutron stars or black holes. This high fraction cannot be explained with current evolutionary calculations. As our analysis assumes synchronization, a better understanding of this process for sdB stars is urgently needed. A larger sample of sdB binaries has to be studied with our method to search for systematic trends and improve statistics.

The presence of such a high fraction of heavy binaries in our samples raises several questions. Is the formation and evolution of sdB stars linked to that of heavy compact objects like neutron stars or black holes? Can sdB stars be used as tracers to find more of these exotic objects? Is there a hidden population of these objects present in our galaxy?

References

Geier, S., Nesslinger, S., Heber, U., Przybilla, N., Napiwotzki, R., & Kudritzki, R.-P. 2007, A&A, 464, 299

Geier, S., Nesslinger, S., Heber, U., Randall, S. K., Edelmann, H., & Green, E. M. 2007, A&A, 477, L13

Han Z., Podsiadlowski P., Maxted P. F. L., Marsh T. R., & Ivanova N. 2002, MNRAS 336, 449

Lemke, M. 1997, A&AS, 122, 285

Maxted P. F. L., Heber U., Marsh T. R., & North R. C. 2001, MNRAS 326, 1391

Table 2. Inclination angles, rotational velocities, companion masses and possible nature of the unseen companions. The lower companion mass corresponds to an sdB of $0.3\,M_\odot$, the higher limit to an sdB of $0.48\,M_\odot$. Binaries up to orbital periods of 1.3 d can be solved consistently under the assumption of synchronization. Empirical and theoretical indications for synchronization are given for individual stars.

System	i [deg]	$v_{\rm rot}$ [km s^{-1}]	$M_{\rm comp}$ [$M_\odot$]	Companion
HE 0532−4503[1,2,3,4]	13 − 17	47	1.40 − 3.60	**NS/BH**
PG 1232−136[1,2,3,4]	14 − 19	25	2.00 − 7.00	**NS/BH**
WD 0107−342[1,2,3,4]	37 − 50	33	0.48 − 0.87	WD
HE 0929−0424[2,4]	23 − 29	18	0.60 − 2.40	**WD/NS/BH**
HE 0230−4323[2,4]	38 − 50	21	0.18 − 0.35	WD/late MS
TONS 183[4]	22 − 29	18	0.60 − 2.40	**WD/NS/BH**
HE 2135−3749[4]	66 − 90	8	0.35 − 0.45	WD/late MS
HE 1421−1206[4]	56 − 90	8	0.15 − 0.30	WD/late MS
HE 1047−0436[4]	62 − 90	7	0.35 − 0.60	WD/late MS
HE 2150−0238[4]	–	–	–	no solution
HE 1448−0510	–	–	–	no solution
WD 0048−202	–	–	–	no solution

[1]Empirical indications for synchronization could be found in subdwarf binaries with longer periods by asteroseismological modelling.
[2]Empirical indications for synchronization could be found in subdwarf binaries with longer periods by detection of ellipsoidal deformation.
[3]Theoretical synchronization timescales are shorter than the average EHB lifetime according to the theory of Zahn (1977).
[4]Theoretical synchronization timescales are shorter than the average EHB lifetime according to the theory of Tassoul & Tassoul (1992).

Napiwotzki, R., Edelmann H., Heber U., Karl, C., Drechsel H., et al. 2001, A&A 378, L17
Napiwotzki, R., Yungelson, L., Nelemans, G., Marsh, T. R., Leibundgut, B., et al. 2004, ASPC, 318, 402
Orosz, J. A., & Wade, R. A. 1999, MNRAS, 310, 773
Randall, S. K., Matthews, J. M., Fontaine, G., Rowe, G., Kuschnig, R., et al. 2005, ApJ, 633, 460
Tassoul J. L., & Tassoul M. 1992, ApJ 395, 259
Zahn J. P. 1977, A&A 57, 383
Zahn J. P. 2005, ASPC, 333, 4